Involvement of NLRP3/Caspase-1/GSDMD-Dependent Pyroptosis In BPA-Induced Apoptosis of Neuroblastoma Cells

Congcong Wang

  South China Normal University - Shipai Campus: South China Normal University

Lei Wang

  South China Normal University - Shipai Campus: South China Normal University

Chengmeng Huang

  South China Normal University - Shipai Campus: South China Normal University

Yungang Liu

  Southern Medical University

Hongxuan Kuang

  South China Normal University - Shipai Campus: South China Normal University

Qihua Pang

  South China Normal University - Shipai Campus: South China Normal University

Hongyu Han

  South China Normal University - Shipai Campus: South China Normal University

Ruifang Fan (✉ 20001047@m.scnu.edu.cn)

  South China Normal University - Shipai Campus: South China Normal University

---

Research

Abstract

Background

Bisphenol A (BPA) is an additive in polycarbonate and epoxy resin particles with endocrine disrupting effects. Previously it has been reported that BPA is neurotoxic *via* induction of cell apoptosis and inflammation, and our recent studies showed that even at nanomolar concentrations BPA accelerated the apoptosis and death of human neuroblastoma cells from both genders, whose mechanisms remain, however, unidentified.

Results

Human neuroblastoma cell lines developed from male and female subjects, IMR-32 and SK-N-SH, respectively, were exposed to BPA at concentrations ranging from 1 nM to 100 μM, for 24 h, with or without epigallocatechin gallate (EGCG, 4 or 8 μM), Z-YVAD-FMK (1 or 10 μM, caspase-1 inhibitor), and ICl182.780 (100 nM or 3 μM, estrogen receptor inhibitor) as modulators. The results showed that BPA nonlinearly upregulated the levels of IL-18, ASC, GSDMD and NLRP3 mRNAs and that of NLRP3, caspase-1, GSDMD and IL-1β proteins in IMR-32 and SK-N-SH cells. Noticeably, the mRNA levels of caspase-1 and IL-1β were changed differently in the two cell lines: the level of caspase-1 mRNA was enhanced in IMR-32 cells but suppressed in SK-N-SH cells, and that of IL-1β was suppressed in IMR-32 cells but enhanced in SK-N-SH cells. The level of GSDMD expression *in situ* was along with the increase in the release of IL-1β, IL-18, caspase-1 and lactate dehydrogenase (LDH). Additionally, Z-YVAD-FMK, ICl182.780 and EGCG significantly reversed the changes of the above mRNAs/proteins induced by BPA. BPA significantly reduced the level of the reactive oxygen species and the rate of LDH leakage and apoptosis, while obviously increased the cell viability and the mitochondrial membrane potential. Meanwhile, Z-YVAD-FMK and ICl182.780 abruptly reduced the levels of Bak1, Bax, Bcl-2 and caspase-3 proteins induced by BPA.

Conclusion

As mediated by the estrogen receptor, BPA may induce the pyroptosis of neuroblastoma cells through NLRP3/caspase-1/GSDMD signaling pathway, and caspase-1-dependent pyroptosis may be involved in BPA-induced apoptosis, which is alleviated by EGCG, an anti-oxidation agent.

Introduction

Bisphenol A (BPA) is a kind of phenolic compound widely used in the production of polycarbonate, polystyrene resin, epoxy resins, electronic equipment and food and beverage packaging (Chang et al., 2015; Staples et al., 1998). In 2015, the global consumption of BPA reached 7.7 million metric tons. Moreover, it will reach up to 10.6 million metric tons by 2022 with an annual growth rate of 4.8% (Wang et al., 2019). The mass production and widespread use of BPA lead to a large amount of release into the environment. Humans are exposed to BPA through ingestion, inhalation and dermal contact (Hines et al.,

2017; Stahlhut et al., 2009). As a result, BPA can be detected in human amniotic fluid, blood, breast milk, placenta, sweat and urine (Shi et al., 2017; Yu et al., 2019).

Multiple *in vivo and in vitro* studies have shown that BPA has neurotoxic effects. For example, BPA exposure decreases the cognitive function, the ability of learning and memory and social response in rats (Negri-Cesi 2015; Zhang et al., 2019; Braun et al., 2017). Studies in the experimental models using primary hippocampus cells, HT-22 cell line and neuroblastoma cells have shown that low-dose BPA exposure induces oxidative stress and increases mitochondrial apoptosis (Meng et al., 2021; Wang et al., 2021; Pang et al., 2019). Epidemiological studies also show that BPA exposure during pregnancy or adolescence may cause neurobehavioral problems in childhood/adolescence (e.g., attention deficit hyperactivity disorder, depression, anxiety, autism spectrum disorders and social cognition/communication deficits) (Miodovnik et al., 2011; Perera et al., 2016; Li et al., 2018). To explore the mechanism of BPA induced neurotoxicity, various attempts have been made and distinct views have been put forward, including the reduction of synaptic plasticity, the inhibition of neurogenesis, the generation of oxidative stress and the induction of autophagy and apoptosis (Santoro et al., 2019). Among them, apoptosis and pyroptosis triggered by oxidative stress are considered as the initial steps of all injuries (Lan et al., 2020; Li et al., 2015; Wang et al., 2019).

Pyroptosis, which is considered to be caspase-1-dependent cell death (Shi et al., 2017), is a newly identified pro-inflammatory form of programmed cell death. Caspase-1 mediated pyroptosis is often activated by cannonical inflammasomes (Zhang et al., 2018). Inflammasomes are large multiprotein complexes that play critical roles in the production of interleukin (IL)-1β and IL-18. Pyrin domain containing 3 (NLRP3) inflammasome, a member of nucleotide binding oligomerization domain-like receptor (NLR) family, is most widely characterized and implicated in inflammatory diseases (Kim et al., 2015). The NLRP3 inflammasome consists of a sensor (NLRP3), an adaptor (ASC, also known as PYCARD) and an effector (pro-caspase-1). ASC is a protein containing pyrin and CARD domain, which promotes the assembly of certain types of inflammasomes. Caspase-1 is activated by upstream inflammasome NLRP3 (Liu et al., 2018; Miao et al., 2011). Once activated, caspase-1 contributes to the maturation of IL-1β and IL-18, and cleaves and activates gasdermin D (GSDMD). GSDMD acts as the pyroptosis executor and finally releases the N-terminal domain (GSDMD-N), which leads to the opening of membrane pores. Subsequently, intracellular contents, such as IL-18, IL-1β and lactate dehydrogenase (LDH), are released into the extracellular environment, eventually leading to the occurrence of pyroptosis (Shi et al., 2017; Strowig et al., 2012). Hence, NLRP3/Caspase-1/GSDMD pathway is very important in regulating pyroptosis.

Our previous study has shown that environmental BPA exposure can induce oxidative stress and mitochondrial apoptosis in different gender neuroblastoma cells (IMR-32 and SK-N-SH cells) (Wang et al., 2021). However, the mechanisms of the pyroptosis in IMR-32 and SK-N-SH cells exposed to low-dose BPA and the relationship between BPA exposure and apoptosis is not known. Hence, this study was conducted to further explore the mechanism of BPA-induced neurotoxicity in IMR-32 and SK-N-SH cells. In this study

we investigated whether low-dose BPA can induce pyroptosis via the NLRP3/Caspase-1/GSDMD signaling pathway with the mediating of estrogen receptor (ER) and its relationship with apoptosis.

Material And Methods

2.1. Cell culture and treatments

IMR-32 and SK-N-SH cells (Shanghai Institute of Cell Biology, Chinese Academy of Sciences) were maintained in the Eagle's minimum essential medium (MEM) (Gibco, 41500034) supplemented with 10% fetal bovine serum (FBS) (Biological Industries, 04-001-1ACS), 1% penicillin-streptomycin (Gibco, 15140163) and 1% sodium pyruvate (Solarbio, P8380), and incubated at 37°C with 5% CO_2. Once the cells confluency reached 70%, they were incubated in the presence or absence of a series of concentrations of BPA (i.e., 0, 1, 10, and 100 nM, and 1, 10, and 100 μM) which cover a spectrum from low to high dose of BPA exposure in humans. The caspase-1 specific inhibitor Z-YVAD-FMK (YVAD) (1 μM or 10 μM, Sigma, SML0429), the ER specific inhibitor ICI182.780 (ICI) (100 nM or 3 μM, Sigma, 129453-61-8), the reactive oxygen species (ROS) inhibitor EGCG (4 μM or 8 μM, Sigma, 989-51-5), were cultured in MEM (Sigma, M3024) containing 10% carbon adsorbed FBS and without phenol red for 1 h and then co-treated with 10 μM or 100 μM BPA for 24 h, respectively.

2.2. Quantitative real-time PCR analysis

Total RNA was extracted from IMR-32 and SK-N-SH cells using Trizol reagent (Takara, Japan). After the measurement of RNA concentration by a NanoDrop Spectrophotometer (NanoDrop-2000, Thermo, USA), 1 μg of total RNA was reversely transcribed into cDNA using a Reverse Transcription Kit (Takara, Japan) for the quantitative real-time PCR (qRT-PCR). A real-time PCR machine (CFX96 Touch, Bio-Rad, USA) was used to perform qRT-PCR with a One Step SYBR® PrimeScript™ RT-PCR Kit II (Takara, Japan). As described in Table 1, the specific primer sequences of duck NLRP3, caspase-1, IL-1β, IL-18, ASC, GSDMD and β-actin were obtained from NCBI GenBank and designed with primer premier 6.0 software. The relative abundance of mRNA was calculated using the $2^{-\Delta\Delta CT}$ method (Livak and Schmittgen, 2001). Results were normalized to the mean of housekeeping gene (i.e., β-actin), and expressed as the relative expression of mRNA levels compared to the control samples.

Table 1
Gene primers sequence and their GenBank accession number

Gene name	Primer sequences (5' to 3')	Accession number
β-actin	Forward: GCACTCTTCCAGCCTTCCTTCC	NM_001101.5
	Reverse: GGCGTACAGGTCTTTGCGGATG	
NLRP3	Forward: GGGACCCAGGGATGAGAGTGTT	NM_001079821.3
	Reverse: TGCTGCTGAGGACCAAGGAGAT	
Caspase-1	Forward: AGACCTCTGACAGCACGTTCCT	NM_033294.4
	Reverse: TCCCACAAATGCCTTCCCGAAT	
IL-1β	Forward: TCCGACCACCACTACAGCAAGG	NM_000576.3
	Reverse: TGGGCAGGGAACCAGCATCTT	
IL-18	Forward: TGGCTGCTGAACCAGTAGAAGA	NM_001386420.1
	Reverse: GGCCGATTTCCTTGGTCAATGA	
ASC	Forward: AGTGGCTGCTGGATGCTCTGT	NM_145182.3
	Reverse: GCACTGCCTGGTACTGCTCATC	
GSDMD	Forward: TGGACCCTAACACCTGGCAGAC	NM_024736.7
	Reverse: AGCACCTCAGTCACCACGTACA	

2.3. Western blot analysis

Western blotting was performed as described previously (Wang et al., 2021). The primary antibodies were anti-NLRP3 (1:1000, Cell Signaling Technology, USA, # 15101S), anti-caspase-1 (1:1000, Cell Signaling Technology, USA, # 3866S), anti-GSDMD (1:1000, Sigma, USA, # HPA044487), anti-IL-1β (1:1000, Cell Signaling Technology, USA, # 12242S), anti-Bak1 (1:1000, Cell Signaling Technology, USA, # 22105S), anti-Bax (1:1000, Cell Signaling Technology, USA, # 2772S), anti-Bcl-2 (1:1000, Sigma, USA, # SAB4500003), anti-caspase-3 (1:1000, Cell Signaling Technology, USA, # 9662S) and β-actin (1:1000, Cell Signaling Technology, USA, # 8457S). The immune complexes with specific proteins were visualized using an ECL detection kit. The densitometry of protein bands was analyzed using a Bio-Rad image analyzer (ChemiDoc Touch, USA). The density ratio of the β-actin band to its corresponding lane was used to correct the amount of protein loading.

2.4. Immunofluorescence staining

IMR-32 and SK-N-SH cells were seeded on 24-well plates containing cell slides for 36 h. Next, cells were washed twice with PBS, fixed with 4% paraformaldehyde for 20 min, and washed three times with PBS. After being permeabilized with 0.1% Triton X-100 for 10 min at room temperature and blocked with 5% bovine serum albumin (BSA) in PBS, cells were incubated with the primary antibodies of GSDMD (1:200,

Sigma, USA, # HPA044487) at 4°C overnight. After being washed for three times with PBS, cells were incubated with the secondary antibodies for 60 min and then the nuclei were re-stained with DAPI (Beyotime, C1005). Slides were visualized using a Leica DM6 fluorescent microscope.

2.5. Enzyme-linked immunosorbent assay

Caspase-1, IL-1β and IL-18 levels in the supernatants of IMR-32 and SK-N-SH cultures were measured by a microtiter plate reader at 450 nm according to the enzyme-linked immunosorbent assay (ELISA) kits (Nanjing Jiancheng Bioengineering Institute, China).

2.6. LDH release assay

Pyroptosis was quantitated by determining the activity of LDH released into the culture medium after various treatments. The LDH activity in the supernatant of each culture was determined by using the LDH cytotoxicity assay kit (Beyotime, C0016), and expressed as a percentage of the total LDH in each cell lysate.

2.7. Cell viability assay

Cell viability was determined by using the Cell Counting Kit-8 (CCK-8, APExBIO, USA). Briefly, IMR-32 and SK-N-SH cells were cultured in 96-well plates. When the cell confluency reached 70–75%, they were treated with BPA and YVAD/or ICI. After 24 h treatments, 10 μL of CCK-8 were added to each well. Then, IMR-32 and SK-N-SH cells were further cultured for 4 h. Finally, the absorbance of each well was read at 450 nm using a microplate reader (PerkinElmer Enspire, USA).

2.8. Flow cytometric analysis

Following various treatments, IMR-32 and SK-N-SH cells were resuspended by using trypsin, and collected by centrifugation. The mitochondrial membrane potential (MMP) and ROS levels were tested using an MMP kit (Beyotime, C2006) and a ROS kit (Beyotime, S0033S). Then cell analysis was performed by flow cytometry (FACS Aria III, BD Biosciences, San Jose, CA, USA) at the 590 or 488 nm excitation wavelength and 525 nm emission wavelength.

2.9. Apoptosis-Hoechst staining

IMR-32 and SK-N-SH cells were seeded on 24-well plates containing cell slides. After 36 h, the cells were fixed with 4% paraformaldehyde for 20 min and stained with Hoechst 33258 for 5 min at room temperature. After being washed three times with PBS, each slide was visualized using a Leica DM6 fluorescent microscope (Lecia, Gemany). Three fields per well/slide were randomly selected for counting the stained cells by using Image J software.

2.10. Statistical analysis

All results are presented as means ± standard deviations of at least three independent experiments. Statistical analysis was completed by GraphPad Prism 6.0 (GraphPad Inc., La Jolla, CA, USA) and SPSS

version 18.0 (SPSS Inc., Chicago, IL, USA). One-way analysis of variance (ANOVA) was used to test the difference between groups, with significance being set at the level of $p < 0.05$.

Results

3.1 Effects of BPA exposure on pyroptosis-related mRNA levels

To test our hypothesis that BPA induces pyroptosis through NLRP3/Caspase-1/GSDMD signaling pathway, the mRNA expressions of NLRP3, GSDMD, ASC, IL-1β, IL-18 and caspase-1 in IMR-32 and SK-N-SH cells were determined (shown in Fig. 1). For IMR-32 cells, mRNA expressions of NLRP3, GSDMD, IL-18 and caspase-1 in the groups with BPA at high concentrations (generally above 1 µM) were significantly increased, as compared with the control group ($p < 0.05$ or 0.01). Interestingly, NLRP3, IL-18 and caspase-1 mRNA expressions in IMR-32 cells treated with 1 nM BPA were still significantly increased ($p < 0.05$). BPA treatments also changed the level of ASC mRNA. Treatment with 1 nM BPA significantly decreased the level of ASC mRNA level while that with 100 µM BPA significantly increased the level ($p < 0.05$); however, IL-1β mRNA level in IMR-32 cells under various treatments was significantly reduced except for that with 1 µM BPA ($p < 0.05$ or 0.01). Moreover, trends of change generally similar to those in IMR-32 cells (described above) were observed in SK-N-SH cells. For example, the mRNA levels of NLRP3, GSDMD, ASC, IL-1β and IL-18 in the treatments with BPA at high concentrations were significantly higher than in the control group. However, as different from the IMR-32 cell line which was developed from the neural tissue of a male subject, BPA treatments significantly decreased the expression of caspase-1 mRNA in the SK-N-SH line (derived from the tissue of a female subject). Moreover, no significant differences were observed between the treatment with 1nM BPA and the control in SK-N-SH cells ($p > 0.05$).

3.2 Effects of BPA exposure on levels of pyroptosis-related proteins

To further confirm whether the gender difference and concentration-dependent effect of BPA at the transcriptional level also exist at the translation level, protein expressions of NLRP3, caspase-1, GSDMD and IL-1β were determined. As shown in Fig. 2A-E, the pyroptosis-related proteins in IMR-32 and SK-N-SH cells generally showed similar trends of change, such as NLRP3, caspase-1, GSDMD and IL-1β, whose levels in IMR-32 cells increased significantly after 24 h exposure to micromolar levels of BPA as compared with the controls ($p < 0.05$ or 0.01). Particularly, 1 nM BPA treatment also led to a significant increase in NLRP3, GSDMD and IL-1β ($p < 0.05$), which is consistent with those variations in mRNA expressions after treatment with BPA. It should be noted that the translation level of IL-1β in IMR-32 cells increased significantly, which was on the contrary of the trend of change at the transcriptional level. Similar to IMR-32 cells, the expressions of NLRP3, caspase-1, GSDMD and IL-1β proteins in SK-N-SH cells treated with 100 nM and/or 1-100 µM BPA for 24 h were significantly higher than those in the control group ($p < 0.05$ or 0.01).

In innate immunity, pyroptosis is executed by the pore-forming protein GSDMD, which is activated by its cleavage mediated by caspase-1 (Shi et al., 2015). Hence, the caspase-1-p20 and GSDMD-N domains of GSDMD were detected by immunoblotting in IMR-32 and SK-N-SH cells (shown in Fig. 2A). Similar to the changes in its transcription, a non-monotonic dose-response relationship between BPA concentrations and the levels of translation of some proteins in neurons, including the caspase-1-p20 and GSDMD-N domains of GSDMD, were observed in both IMR-32 and SK-N-SH cells after 24 h treatments. To further verification the occurrence of pyroptosis, we used immunofluorescence staining to analyze the localization and expression of GSDMD (Fig. 2F). The increase of green fluorescence further confirmed that BPA induced pyroptosis in IMR-32 and SK-N-SH cells.

3.3 Effects of BPA on the contents of inflammatory factors in the supernatants of IMR-32 and SK-N-SH cells and the cell morphology

Next, the effects of BPA on the levels of inflammatory factors (LDH, caspase-1, IL-1β and IL-18) in the cell supernatants were studied. As shown in Fig. 3 **(B-E)**, after 24 h treatment, BPA at various concentrations (1 nM, 100 nM and 1-100 μM) significantly increased the concentrations of inflammatory factors (i.e., LDH, caspase-1, IL-1β and IL-18) in the supernatant of IMR-32 cells ($p < 0.05$ or 0.01). In SK-N-SH cells, these inflammatory factors were also significantly increased after 24 h exposure to 100 nM, 1 μM, or 100 μM of BPA. The relationship of BPA concentration and LDH, caspase-1, IL-1β and IL-18 levels of IMR-32 and SK-N-SH cells were not linear, but non-monotonic. Even low dose of BPA (i.e., nM) can also induce the pyroptosis of IMR-32 and SK-N-SH cells. The ballooning of the cell membrane further confirmed a characteristic morphological of pyroptosis induced by BPA (Fig. 3A). It showed that the BPA-induced pyroptosis formed a gap, which caused the release of LDH and inflammatory factors in IMR-32 and SK-N-SH cells.

3.4 Inhibition of the pyrotosis of IMR-32 and SK-N-SH cells exposed to BPA by EGCG

In our previous studies, we found that ROS production played an important role in the BPA-induced apoptosis in IMR-32 and SK-N-SH cells by adding EGCG (an antioxidant) (Wang et al., 2021). We hypothesize that ROS also plays a similar role in the BPA-induced pyroptosis by detecting the expression levels of factors related to NLRP3/Caspase-1/GSDMD pathway after adding EGCG. Results showed that EGCG significantly attenuated the BPA-induced effects, including the increasing of LDH, caspase-1, IL-1β and IL-18 contents in cell supernatants, the rising of mRNA levels of NLRP3, caspase-1, GSDMD, ASC, IL-1β and IL-18 and the increasing of protein levels of caspase-1, GSDMD, IL-1β and NLRP3 in IMR-32 / SK-N-SH cells, the decreasing of IL-1β mRNA level in IMR-32 cells, the reduction of caspase-1 mRNA level in SK-N-SH cells, as well as the reducing of MMP level in IMR-32 and SK-N-SH cells (Fig. 4).

3.5 Attenuation of pyroptosis and mitochondrial apoptosis in IMR-32 and SK-N-SH cells exposed to BPA by caspase-1 deletion

To verify the role of caspase-1 in the BPA-induced pyroptosis and explore the relationship between apoptosis and pyroptosis, IMR-32 and SK-N-SH cells were pre-treated and co-treated with YVAD. YVAD is a potent cell permeable and irreversible Caspase-1 inhibitor, which can reduce the activation of caspase-1, and then inhibit pyroptosis. As shown in Fig. 5A-B **and E**, the MMP and the cell viability of IMR-32 and SK-N-SH cells in the BPA-treated groups dramatically decreased compared with the control groups ($p < 0.05$ or $p < 0.001$). But after the co-treatment with YVAD, there was no significant difference of MMP and cell viability between the YVAD + BPA group and the control group ($p > 0.5$). In the meantime, significant difference of the cell viability existed between the BPA group and the YVAD + BPA group in SK-N-SH cells ($p < 0.001$). Additionally, the results showed that the rates of apoptosis and the contents of LDH of the BPA-treated groups in IMR-32 and SK-N-SH cells significantly increased compared to those of the control group ($p < 0.05$ or $p < 0.01$). But in the BPA + YVAD group, the rates of apoptosis and the contents of LDH decreased and were significantly lower than those in the BPA group ($p < 0.001$) (Fig. 5D, C and F). There was no significant difference of above indicators between the control and the YVAD group ($p > 0.05$).

Similar effects of YVAD on the mRNA levels (i.e., NLRP3, GSDMD, ASC, IL-1β, IL-18 and caspase-1) and the protein levels (i.e., Bcl-2, Bax, Bak1, caspase-3, NLRP3, caspase-1, GSDMD and IL-1β) were observed in IMR-32 and SK-N-SH cells again (Fig. 5G-L). All results suggest that caspase-1 is actually involved in the pyroptosis of IMR-32 and SK-N-SH cells. These data demonstrate that the BPA-induced pyroptosis in IMR-32 and SK-N-SH cells is mainly caspase-1-dependent and related to apoptosis.

3.6 Induction of ROS production, apoptosis and pyroptosis by BPA via actions on ER

Since BPA can activate the ER, we investigated whether the observed effects of BPA on IMR-32 and SK-N-SH cells were due to the estrogenic effect of BPA. Hence, ICI, a compound which can block the ER pathway, was used to verify it. Before cells were co-treated with 10 μM or 100 μM BPA and ICI for 24 h, IMR-32 and SK-N-SH cells were pretreated with 100 nM and 3 μM ICI for 1 h. As described in Fig. 6A-J, BPA significantly elevated the levels of ROS, the conttent of LDH and the rate of apoptosis, the mRNA expressions of NLRP3, GSDMD, ASC and IL-18, the protein expressions of Bax, Bak1, caspase-3, caspase-1, NLRP3, GSDMD and IL-1β, and reduced the Bcl-2 protein expressions in IMR-32 and SK-N-SH cells. Moreover, the mRNA level of intracellular caspase-1 in IMR-32 cells and the mRNA level of IL-1β in SK-N-SH cells were also significantly upregulated, while the expression of IL-1β mRNA in IMR-32 cells and the expression of caspase-1 mRNA in SK-N-SH cells were significantly inhibited ($p < 0.05$ or $p < 0.01$ or $p < 0.001$). Finally, BPA led to a decrease of cell viability. However, ICI could significantly ameliorate the changes of the above indicators caused by BPA. The activation of caspase-1 and the cleavage of GSDMD were also significantly inhibited by ICI.

Discussion

4.1 BPA may induce pyroptosis by NLRP3/Caspase-1/GSDMD signaling pathway

Pyroptosis is a newly identified form of inflammatory cell death triggered by caspase-1, which is characterized by caspase-1-dependence, the accumulation of GSDMD fragments, the formation of membrane pores and the leakage of intracellular contents, such as IL-18, IL-1β, LDH, etc. (Pi et al., 2021). Studies have shown that pyroptosis is involved in various diseases, particularly neurodegenerative diseases (Voet et al., 2019; Zhao et al., 2019). It is reported that polystyrene microplastics, which continuously pollute the environment, can induce pyroptosis and apoptosis of ovarian granulosa cells via the NLRP3/caspase-1 signaling pathway triggered by oxidative stress (Hou et al., 2021). Moreover, the activation of NLRP3 plays an important role in caspase-1-dependent pyroptosis. For example, one study has shown that the activation of NLRP3 is critical for the cell pyroptosis induced by propofol (Sun et al., 2019). Caspase-1 is responsible to transform pro-IL-1β to IL-1β (the active form), which is thus named IL-1β converting enzyme (Zhao et al., 2012). Activated caspase cleaves the connection between the *N*-terminal and *C*-terminal domains of GSDMD protein and releases the active *N*-terminal domain, which destroys the cell membrane and causes pyroptosis (Ding et al., 2016). In this study, BPA treatments can not only significantly change the mRNA levels of NLRP3, GSDMD, ASC, IL-1β, IL-18 and caspase-1 and the protein levels of Bcl-2, Bax, Bak1, caspase-3, NLRP3, caspase-1, GSDMD and IL-1β, but also increase the secretion of IL-1β, IL-18, caspase-1 and LDH in neuroblastoma cells, especially in IMR-32 cells from male. All results suggest that BPA induces pyroptosis of nervous cells, and male IMR-32 cells are more susceptible to BPA than female SK-N-SH cells. Moreover, even 1 nM BPA treatments can lead to the similar effects and consequently promote the pyroptosis of IMR-32 cells. These results suggest that BPA treatments can potently induce pyroptosis of IMR-32 and SK-N-SH cells. In the same time, our study also shows that the BPA-induced pyroptosis not only triggers nervous cell death but also mediates the releases of IL-1β, IL-18, caspase-1 and LDH, which will lead to an excessive proinflammatory process. Based on the above factors, LDH release is considered to be one of the main characteristics of pyroptosis (Fink et al., 2008). As an inhibitor of pyroptosis, YVAD is reported to restrain the caspase-1 activation, reduce the secretion of IL-1β and IL-18 and suppress the occurrence of pyroptosis in cells (Yue et al., 2019; Zamani et al., 2020). In this study, the caspase-1 mRNA and protein levels were significantly inhibited after YVAD treatment as expected, which further confirms that YVAD inhibits the pyroptosis of IMR-32 and SK-N-SH cells by inhibiting the activation of caspase-1. Simultaneously, the differences of mRNA expressions (i.e., NLRP3, GSDMD, ASC, IL-1β and IL-18), protein expressions (i.e., NLRP3, GSDMD and IL-1β) and GSDMD fluorescence expression between the BPA-treated group and the BPA + YVAD treated group suggest that BPA can induce pyroptosis in IMR-32 and SK-N-SH cells via NLRP3/Caspase-1/GSDMD signaling pathway.

Our previous studies has shown that BPA can promote ROS production, leading to oxidative stress and apoptosis in IMR-32 and SK-N-SH cells (Wang et al., 2021). ROS is involved in pyroptosis and has a

significant action in regulating pyroptosis, which has been confirmed in many studies (Chen et al., 2016; Zhang et al., 2021). Excessive ROS may activate the NLRP3 inflammasome signaling pathway (Sun et al., 2019). In addition, ROS can mediate the NLRP3/Caspase-1/GSDMD signaling pathway involved in the process of cytotoxicity (Yang et al., 2020). Therefore, we speculated that ROS might also be involved in the BPA-induced pyroptosis of IMR-32 and SK-N-SH cells via the NLRP3/Caspase-1/GSDMD pathway. In our study, if cells were co-treated with BPA and EGCG, the differential expressions of mRNA (i.e., NLRP3, GSDMD, ASC, IL-1β, IL-18 and caspase-1) and proteins (i.e., NLRP3, caspase-1, GSDMD and IL-1β) in IMR-32 and SK-N-SH cells between the BPA-treated groups and the BPA + EGCG-treated groups were reduced or eliminated. At the same time, the secretion of IL-1β, IL-18, caspase-1 and LDH were also reduced. In addition, the level of MMP was increased. As inflammasomes induce the maturation and the release of IL-1β and IL-18, we preliminarily speculate that the BPA-induced ROS activate the NLRP3 inflammasome, and then resulting in pyroptosis. As a ROS scavenger, EGCG can inhibit caspase-1-dependent pyroptosis in IMR-32 and SK-N-SH cells.

4.2 Pyroptosis of neuroblastoma cells by BPA contributes to apoptosis

Pyroptosis is a caspase-1-dependent form of programmed inflammatory cell death. Apoptosis is a caspase-3-dependent and non-inflammatory programmed form (Rogers et al., 2017), regulated by anti-apoptotic and pro-apoptotic families (i.g., caspase family and Bcl-2 family) (Siddiqui et al., 2015). Caspase-3 is often activated by the death receptor mediated apoptotic pathway through the mitochondrial apoptotic pathway (Li and Yuan, 2008), which is controlled by the Bcl-2 family proteins. The activation of two Bcl-2 family members (i.e., Bak and Bax) can form pores on the mitochondrial outer-membrane, resulting in the release of mitochondrial inter-membrane components, and finally activate the occurrence of caspase cascade (Czabotar et al., 2014; Degterev and Yuan, 2008; Delbridge et al., 2016). However, pyroptosis can also be induced by pro-apoptotic caspase-3 (Rogers et al., 2017; Wang et al., 2017). Therefore, understanding the relationship of pyroptosis with apoptosis is helpful to clarify the mechanism of BPA apoptosis.

Environmental pollutants are considered an important factor causing pyroptosis and apoptosis (Yu et al., 2021; Zhang et al., 2021). Moreover, cell pyroptosis has been proved to promote cell apoptosis (Shi et al., 2017). Pi et al. reported that molybdenum induced pyroptosis in duck renal tubular epithelial cells and YVAD reduced the molybdenum-induced apoptosis (Pi et al., 2021). We hypothesized that the relationship of apoptosis and pyroptosis in nervous cells induced by BPA might be similar to the previous reports. In our study, YVAD was used as a caspase-1 inhibitor to explore the relationship between the BPA-induced pyroptosis and apoptosis by detecting protein levels of Bcl-2, Bak-1, Bax and caspase-3, MMP and apoptosis ratio. Bak-1 and Bax can promote apoptosis (Shi et al., 2010). Bcl-2 can inhibit apoptosis, which is mainly located on the outer membrane of the mitochondria and regulates apoptosis through mitochondrial pathway (Birkinshaw and Czabotar, 2017). Caspase-3 is the executor caspase of apoptosis. MMP is a vital marker of intrinsic apoptosis (Park et al., 2020). Our results showed that protein levels of Bak-1, Bax and caspase-3 in the 10 μM or the 100 μM BPA-treated groups were significantly

higher than those in the control group, but the protein level of Bcl-2 demonstrated the opposite trend in IMR-32 (or SK-N-SH) cells. Further studies showed that BPA treatments could decrease MMP and increase apoptosis ratio and LDH level. Moreover, YVAD could significantly improve the changes of apoptosis-related indicators induced by BPA. These results suggest that YVAD can decrease the BPA-induced apoptosis in neuroblastoma cells. Moreover, the activation of caspase-1 is involved in the BPA-induced apoptosis. Hence, we can conclude that apoptosis is related with pyroptosis in the BPA-induced neurotoxicity, and the inhibition of caspase-1 dependent pyroptosis may attenuate the BPA-induced apoptosis in neuroblastoma cells.

4.3 BPA induces damages in neuroblastoma cells in a nonmonotonic and gender-specific manner

In this study, we used IMR-32 and SK-N-SH cells as the model to investigate the gender-dependent neurotoxicity induced by various concentrations of BPA. Interestingly, a non-monotonic relationship between the BPA concentrations and cytotoxic effects was observed. In particular, low-dose BPA treatment showed more obvious cytotoxicity than medium or high dose. There was an inverted U-shaped curve between BPA exposure concentration and cytotoxicity, which may be attributed to the exogenous endocrine disrupting effects of BPA. Our results are in accordance with the previous studies that low-dose BPA or bisphenol S can cause significant impacts on rats, while the middle-dose BPA has no obvious effects (da Silva et al., 2019; Zhang et al., 2019). In general, concentrations used to assess toxic effects of pollutants often range from low to high doses. However, only high concentration exposure is used in the study of molecular mechanism if the dose-effect response is linear. Our study showed that it is important to set the appropriate concentration range of BPA according to the toxic effect to study its corresponding toxic mechanism. Otherwise, improper concentration selection will lead to meaningless mechanism or opposite results because its non-linear relationships between dose and effects. It is easier to draw meaningful conclusions by selecting concentrations of toxic effects.

As an environmental endocrine disruptor, BPA has been shown to activate several types of receptors, including ER (Perera et al., 2017; Pinto et al., 2019). Although our *in vitro* studies have shown that BPA treatment can lead to apoptosis and pyroptosis in different gender nervous cells, and further confirmed the previous *in vivo* data that BPA can gender-dependently disrupt dendritic development and neurotransmitter homeostasis in the rat hippocampus (Zhang et al., 2019), the exact mechanism of BPA gender-specific induction of apoptosis and pyroptosis of neuroblastoma cells remains unclear. In this study, at the transcriptional level, our results showed that the expression trends of IL-1β and caspase-1 levels were opposite in male and female neuroblastoma cells, while the expression trends at the translation level were consistent between both gender cells. And then we observed that the BPA-induced apoptosis and pyroptosis in IMR-32 and SK-N-SH cells were significantly attenuated after the ICI (an ER inhibitor) pretreatments. Therefore, BPA may induce apoptosis and pyroptosis of nervous cells through ER. The distribution and content of ER in the body may be related to the higher effects of BPA on males. Bisphenol AF, an analogue of BPA, is reported to promote the ER activation and induce apoptosis in some cell lines (Huang et al., 2021; Kojima et al., 2019). When the secretion of estrogen is reduced and the

expression of ER is low, women are more prone to vascular damage (Trenti et al., 2018). BPA exposure resulted in a significant down-regulation of estrogen receptor β (ER_β) in male hippocampus, but not in female hippocampus (Xu et al., 2015). Therefore, the role of exogenous estrogens (including BPA) in ER activation and function (i.g., the regulation of ROS generation, apoptosis and pyroptosis) still needs to be further clarified by primary cells or animal experiments.

Conclusions

BPA may potently induce the pyroptosis of neuroblastoma cells through the NLRP3/caspase-1/GSDMD signaling pathway, in a ER-dependent, gender-specific and non-monotonic manner, which is alleviated by antioxidation treatment. Male neuroblastoma cells seem to be more susceptible to BPA than female ones.

Declarations

Acknowledgements

Conflict of interest statement

On behalf of the authors of this paper, I hereby certify that all actual or potential competing financial interests have been declared and that the authors' freedom to design, conduct, interpret, and publish research is not compromised by any controlling sponsor as a condition of review and publication.

References

1. Birkinshaw RW, Czabotar PE. The Bcl-2 family of proteins and mitochondrial outer membrane permeabilisation. Semin Cell Dev Biol. 2017;72:152–62. http://dx.doi.org/10.1016/j.semcdb.2017.04.001.

2. Braun JM, Muckle G, Arbuckle T, Bouchard MF, Fraser WD, Ouellet E, Seguin JR, Oulhote Y, Webster GM, Lanphear BP. 2017. Associations of prenatal urinary bisphenol A concentrations with child behaviors and cognitive abilities. Environ Health Perspect 125(6). http://dx.doi.org/Artn 06700810.1289/Ehp984.

3. Chang TJ, Fan CY, Man Y, Zhou JH, Jing YP. Bisphenol A affects germination and tube growth in Picea meyeri pollen through modulating Ca^{2+} flux and disturbing actin-dependent vesicular trafficking during cell wall construction. Plant Physiol Bioch. 2015;94:216–24. http://dx.doi.org/10.1016/j.plaphy.2015.06.010.

4. Chen HY, Lu YH, Cao ZW, Ma QL, Pi HF, Fang YL, Yu ZP, Hu HX, Zhou Z. Cadmium induces NLRP3 inflammasome-dependent pyroptosis in vascular endothelial cells. Toxicol Lett. 2016;246:7–16.

http://dx.doi.org/10.1016/j.toxlet.2016.01.014.

5. Czabotar PE, Lessene G, Strasser A, Adams JM. Control of apoptosis by the BCL-2 protein family: implications for physiology and therapy. Nat Rev Mol Cell Biol. 2014;15(1):49–63. http://dx.doi.org/10.1038/nrm3722.

6. da Silva BS, Pietrobon CB, Bertasso IM, Lopes BP, Carvalho JC, Peixoto-Silva N, Santos TR, Claudio-Neto S, Manhaes AC, Oliveira E, de Moura EG, Lisboa PC. Short and long-term effects of bisphenol S (BPS) exposure during pregnancy and lactation on plasma lipids, hormones, and behavior in rats. Environ Pollution. 2019;250:312–22. http://dx.doi.org/10.1016/j.envpol.2019.03.100.

7. Degterev A, Yuan JY. Expansion and evolution of cell death programmes. Nat Rev Mol Cell Biol. 2008;9(5):378–90. http://dx.doi.org/10.1038/nrc.2015.17.

8. Delbridge ARD, Grabow S, Strasser A, Vaux DL. Thirty years of Bcl-2: translating cell death discoveries into novel cancer therapies. Nat Rev Cancer. 2016;16(2):99–109. http://dx.doi.org/10.1038/nrc.2015.17.

9. Ding JJ, Wang K, Liu W, She Y, Sun Q, Shi JJ, Sun HZ, Wang DC, Shao F. Pore-forming activity and structural autoinhibition of the gasdermin family. Nature. 2016;535(7610):111–6. http://dx.doi.org/10.1038/nature18590.

10. Fink SL, Bergsbaken T, Cookson BT. Anthrax lethal toxin and salmonella elicit the common cell death pathway of Caspase-1-dependent pyroptosis via distinct mechanisms. P Natl Acad Sci USA. 2008;105(11):4312–7. http://dx.doi.org/10.1073/pnas.0707370105.

11. Hines CJ, Jackson MV, Deddens JA, Clark JC, Ye XY, Christianson AL, Meadows JW, Calafat AM. 2017. Urinary Bisphenol A (BPA) concentrations among workers in industries that manufacture and use BPA in the USA. Ann Work Expos Heal 61(2): 164–82. http://dx.doi.org/DOI 10.1093/annweh/wxw021.

12. Hou JY, Lei ZM, Cui LL, Hou Y, Yang L, An R, Wang QM, Li SD, Zhang HQ, Zhang LS. Polystyrene microplastics lead to pyroptosis and apoptosis of ovarian granulosa cells via NLRP3/Caspase-1 signaling pathway in rats. Ecotoxicol Environ Saf. 2021;212:112012. http://dx.doi.org/10.1016/j.ecoenv.2021.112012.

13. Huang MQ, Li XJ, Jia SJ, Liu S, Fu L, Jiang X, Yang M. Bisphenol AF induces apoptosis via estrogen receptor beta (ERbeta) and ROS-ASK1-JNK MAPK pathway in human granulosa cell line KGN. Environ Pollut. 2021;270:116051. http://dx.doi.org/10.1016/j.envpol.2020.116051.

14. Kim RY, Pinkerton JW, Gibson PG, Cooper MA, Horvat JC, Hansbro PM. Inflammasomes in copd and neutrophilic asthma. Thorax. 2015;70(12):1199–201. http://dx.doi.org/10.1136/thoraxjnl-2014-206736.

15. Kojima H, Takeuchi S, Sanoh S, Okuda K, Kitamura S, Uramaru N, Sugihara K, Yoshinari K. Profiling of bisphenol A and eight its analogues on transcriptional activity via human nuclear receptors. Toxicology. 2019;413:48–55. http://dx.doi.org/10.1016/j.tox.2018.12.001.

16. Lan M, Zhang Y, Wan X, Pan MH, Xu Y, Sun SC. 2020. Melatonin ameliorates ochratoxin a-induced oxidative stress and apoptosis in porcine oocytes. Environ Pollut 256. http://dx.doi.org/ARTN

11337410.1016/j.envpol.2019.113374.

17. Li J, Yuan J. Caspases in apoptosis and beyond. Oncogene. 2008;27(48):6194–206. http://dx.doi.org/10.1038/onc.2008.297.

18. Li LL, Tan J, Miao YY, Lei P, Zhang Q. ROS and autophagy: interactions and molecular regulatory mechanisms. Cell Mol Neurobiol. 2015;35(5):615–21. http://dx.doi.org/10.1007/s10571-015-0166-x.

19. Liu XM, Zhong LB, Meng J, Wang F, Zhang JJ, Zhi YY, Zeng LZ, Tang XJ, Xu JM. A multi-medium chain modeling approach to estimate the cumulative effects of cadmium pollution on human health. Environ Pollut. 2018;239:308–17. http://dx.doi.org/10.1016/j.envpol.2018.04.033.

20. Livak KJ, Schmittgen TD. Analysis of relative gene expression data using real-time quantitative PCR and the 2(T)(-Delta Delta C) method. Methods. 2001;25(4):402–8. http://dx.doi.org/10.1006/meth.2001.1262.

21. Meng LX, Liu J, Wang CC, Ouyang ZD, Kuang JH, Pang QH, Fan RF. Sex-specific oxidative damage effects induced by BPA and its analogs on primary hippocampal neurons attenuated by EGCG. Chemosphere. 2021;264(1):128450. https://doi.org/10.1016/j.chemosphere.2020.128450.

22. Miao EA, Rajan JV, Aderem A. Caspase-1-induced pyroptotic cell death. Immunol Rev. 2011;243:206–14. http://dx.doi.org/10.1111/j.1600-065X.2011.01044.x.

23. Miodovnik A, Engel SM, Zhu C, Ye X, Soorya LV, Silva MJ, Calafat AM, Wolff MS. Endocrine disruptors and childhood social impairment. Neurotoxicology. 2011;32(2):261–7. http://dx.doi.org/10.1016/j.neuro.2010.12.009.

24. Negri-Cesi P. 2015. Bisphenol A interaction with brain development and functions. Dose-Response 13(2). http://dx.doi.org/Artn 1559325815590394 10.1177/1559325815590394.

25. Park W, Lim W, Park S, Whang KY, Song G. 2020. Exposure to etoxazole induces mitochondria-mediated apoptosis in porcine trophectoderm and uterine luminal epithelial cells. Environ Pollut 257: 1–11. http://dx.doi.org/ARTN 11348010.1016/j.envpol.2019.113480.

26. Perera F, Nolte ELR, Wang Y, Margolis AE, Calafat AM, Wang S, Garcia W, Hoepner LA, Peterson BS, Rauh V, Herbstman J. Bisphenol A exposure and symptoms of anxiety and depression among inner city children at 10–12 years of age. Environ Res. 2016;151:195–202. http://dx.doi.org/10.1016/j.envres.2016.07.028.

27. Perera L, Li Y, Coons LA, Houtman R, van Beuningen R, Goodwin B, Auerbach SS, Teng CT. Binding of bisphenol A, bisphenol AF, and bisphenol S on the androgen receptor: Coregulator recruitment and stimulation of potential interaction sites. Toxicol in Vitro. 2017;44:287–302. http://dx.doi.org/10.1016/j.tiv.2017.07.020.

28. Pi SX, Nie GH, Wei ZJ, Yang F, Wang C, Xing CH, Hu GL, Zhang CY. Inhibition of ROS/NLRP3/Caspase-1 mediated pyroptosis alleviates excess molybdenum-induced apoptosis in duck renal tubular epithelial cells. Ecotoxicol Environ Saf. 2021;208:111528. http://dx.doi.org/10.1016/j.ecoenv.2020.111528.

29. Pinto C, Hao R, Grimaldi M, Thrikawala S, Boulahtouf A, Ait-Aissa S, Brion F, Gustafsson JA, Balaguer P, Bondesson M. Differential activity of BPA, BPAF and BPC on zebrafish estrogen receptors in vitro

and in vivo. Toxicol Appl Pharmacol. 2019;380:114709. http://dx.doi.org/10.1016/j.taap.2019.114709.

30. Rogers C, Fernandes-Alnemri T, Mayes L, Alnemri D, Cingolani G, Alnemri ES. 2017. Cleavage of DFNA5 by caspase-3 during apoptosis mediates progression to secondary necrotic/pyroptotic cell death. Nat Communications 8: 14128. http://dx.doi.org/ARTN 1412810.1038/ncomms14128.

31. Santoro A, Chianese R, Troisi J, Richards S, Nori SL, Fasano S, Guida M, Plunck E, Viggiano A, Pierantoni R, Meccariello R. Neuro-toxic and Reproductive Effects of BPA. Curr Neuropharmacol. 2019;17(12):1109–32. http://dx.doi.org/10.2174/1570159x17666190726112101.

32. Shi JJ, Gao WQ, Shao F. Pyroptosis: Gasdermin-mediated programmed necrotic cell Death. Trends Biochem Sci. 2017;42(4):245–54. http://dx.doi.org/10.1016/j.tibs.2016.10.004.

33. Shi JJ, Zhao Y, Wang K, Shi XY, Wang Y, Huang HW, Zhuang YH, Cai T, Wang FC, Shao F. Cleavage of GSDMD by inflammatory caspases determines pyroptotic cell death. Nature. 2015;526(7575):660–5. http://dx.doi.org/10.1038/nature15514.

34. Shi L, Chen JA, Yang JA, Pan TH, Zhang SG, Wang ZM. MiR-21 protected human glioblastoma U87MG cells from chemotherapeutic drug temozolomide induced apoptosis by decreasing Bax/Bcl-2 ratio and caspase-3 activity. Brain Res. 2010;1352:255–64. http://dx.doi.org/10.1016/j.brainres.2010.07.009.

35. Shi WB, Wang R, Niu SB, Li YM, Ma CL, Zhang GZ, Cong B. Dynamaic changes of proliferation and apoptosis in rat retina development. Int J Exp Pathol. 2017;10(12):11679–84. https://www.ncbi.nlm.nih.gov/pubmed/31966527.

36. Siddiqui WA, Ahad A, Ahsan H. The mystery of BCL2 family: Bcl-2 proteins and apoptosis: an update. Arch Toxicol. 2015;89(3):289–317. http://dx.doi.org/10.1007/s00204-014-1448-7.

37. Stahlhut RW, Welshons WV, Swan SH. Bisphenol A data in nhanes suggest longer Than expected half-Life, substantial nonfood exposure, or both. Environ Health Perspect. 2009;117(5):784–9. http://dx.doi.org/10.1289/ehp.0800376.

38. Staples CA, Dorn PB, Klecka GM, O'Block ST, Harris LR. 1998. A review of the environmental fate, effects, and exposures of Bisphenol A. Chemosphere 36(10): 2149–2173. http://dx.doi.org/Doi10.1016/S0045-6535(97)10133-3.

39. Strowig T, Henao-Mejia J, Elinav E, Flavell R. Inflammasomes in health and disease. Nature. 2012;481(7381):278–86. http://dx.doi.org/10.1038/nature10759.

40. Sun LB, Ma W, Gao WL, Xing YM, Chen LX, Xia ZY, Zhang ZJ, Dai ZL. 2019. Propofol directly Induces caspase-1-dependent macrophage pyroptosis through the NLRP3-ASC inflammasome. Cell Death Dis 10(8):542. http://dx.doi.org/ARTN 54210.1038/s41419-019-1761-4.

41. Trenti A, Tedesco S, Boscaro C, Trevisi L, Bolego C, Cignarella A. 2018. Estrogen, angiogenesis, immunity and cell metabolism: solving the puzzle. Int J Mol Sci 19(3): 859. http://dx.doi.org/ARTN 85910.3390/ijms19030859.

42. Voet S, Srinivasan S, Lamkanfi M, van Loo G. Inflammasomes in neuroinflammatory and neurodegenerative diseases. EMBO Mol Med. 2019;11(6):1–16.

http://dx.doi.org/10.15252/emmm.201810248.

43. Wang CC, He JY, Xu TF, Han HY, Zhu ZM, Meng LX, Pang QH, Fan RF. Bisphenol A(BPA), BPS and BPB-induced oxidative stress and apoptosis mediated by mitochondria in human neuroblastoma cell lines. Ecotoxicol Environ Saf. 2021;207:111299. http://dx.doi.org/10.1016/j.ecoenv.2020.111299.

44. Wang HG, Chang L, Aguilar JS, Dong SJ, Hong YL. Bisphenol-A exposure induced neurotoxicity in glutamatergic neurons derived from human embryonic stem cells. Environ Int. 2019;127:324–32. http://dx.doi.org/10.1016/j.envint.2019.01.059.

45. Wang YF, Shi PL, Chen Q, Huang Z, Zou DY, Zhang JZ, Gao X, Lin ZY. Mitochondrial ROS promote macrophage pyroptosis by inducing GSDMD oxidation. J Mol Cell Biol. 2019;11(12):1069–82. http://dx.doi.org/10.1093/jmcb/mjz020.

46. Wang YP, Gao WQ, Shi XY, Ding JJ, Liu W, He HB, Wang K, Shao F. Chemotherapy drugs induce pyroptosis through caspase-3 cleavage of a gasdermin. Nature. 2017;547(7661):99–103. http://dx.doi.org/10.1038/nature22393.

47. Xu XH, Dong FN, Yang YL, Wang Y, Wang R, Shen XY. Sex-specific effects of long-term exposure to bisphenol-A on anxiety- and depression-like behaviors in adult mice. Chemosphere. 2015;120:258–66. http://dx.doi.org/10.1016/j.chemosphere.2014.07.021.

48. Yang Y, Liu PY, Bao W, Chen SJ, Wu FS, Zhu PY. 2020. Hydrogen inhibits endometrial cancer growth via a ROS/NLRP3/Caspase-1/GSDMD-mediated pyroptotic pathway. BMC Cancer 20(1). http://dx.doi.org/ARTN 2810.1186/s12885-019-6491-6.

49. Yu LD, Das P, Vall AJ, Yan Y, Gao XH, Sifre MI, Bortner CD, Castro L, Kissling GE, Moore AB, Dixon D. Bisphenol A induces human uterine leiomyoma cell proliferation through membrane-associated ERalpha36 via nongenomic signaling pathways. Mol Cell Endocrinol. 2019;484:59–68. http://dx.doi.org/10.1016/j.mce.2019.01.001.

50. Yu YJ, Chen HB, Hua X, Wang ZD, Li LZ, Li ZR, Xiang MD, Ding P. Long-term toxicity of lindane through oxidative stress and cell apoptosis in caenorhabditis elegans. Environ Pollut. 2021;272:116036. http://dx.doi.org/10.1016/j.envpol.2020.116036.

51. Yue RC, Lu SZ, Luo Y, Zeng J, Liang H, Wang XB, Qin D, Yang XL, Hu HX, Zeng CY. Effect of NLRP3 mediated pyroptosis in myocardial cells undergoing hypoxia/deoxygenation injury. Zhonghua Xin Xue Guan Bing Za Zhi. 2019;47(6):471–8. http://dx.doi.org/10.3760/cma.j.issn.0253-3758.2019.06.009.

52. Zamani S, Morand EF, Flynn JK. Assays for Inducing and Measuring Cell Death to Detect Macrophage Migration Inhibitory Factor (MIF) Release. Methods Mol Biol. 2020;2080:173–83. http://dx.doi.org/10.1007/978-1-4939-9936-1_15.

53. Zhang CY, Lin TJ, Nie GH, Hu RM, Pi SX, Wei ZJ, Wang C, Xing CH, Hu GL. Cadmium and molybdenum co-induce pyroptosis via ROS/PTEN/PI3K/AKT axis in duck renal tubular epithelial cells. Environ Pollut. 2021;272:116403. http://dx.doi.org/10.1016/j.envpol.2020.116403.

54. Zhang HB, Kuang HX, Luo YF, Liu SH, Meng LX, Pang QH, Fan RF. 2019. Low-dose bisphenol A exposure impairs learning and memory ability with alterations of neuromorphology and

neurotransmitters in rats. Sci Total Environ 697: 134036. http://dx.doi.org/ARTN 13403610.1016/j.scitotenv.2019.134036.

55. Zhang L, Ding F, Wang RJ, Wu X, Wan Y, Hu JY, Wu Q. Involvement of mitochondrial fission in renal tubular pyroptosis in mice exposed to high and environmental levels of glyphosate combined with hard water. Environ Pollut. 2021;283:117082. http://dx.doi.org/10.1016/j.envpol.2021.117082.

56. Zhang YY, Chen X, Gueydan C, Han JH. Plasma membrane changes during programmed cell deaths. Cell Res. 2018;28(1):9–21. http://dx.doi.org/10.1038/cr.2017.133.

57. Zhao HJ, Yan HB, Yamashita S, Li WZ, Liu C, Chen Y, Zhou P, Chi YP, Wang SP, Zhao B, Song L. 2012. Acute ST-Segment Elevation Myocardial Infarction is Associated with Decreased Human Antimicrobial Peptide LL-37 and Increased Human Neutrophil Peptide-1 to 3 in Plasma. J Atheroscler Thromb 19(4): 357–68. http://dx.doi.org/DOI 10.5551/jat.10108.

58. Zhao NN, Sun CX, Zheng M, Liu S, Shi R. 2019. Amentoflavone suppresses amyloid beta 1–42 neurotoxicity in alzheimer's disease through the inhibition of pyroptosis. Life Sci 239: 117043 http://dx.doi.org/ARTN 11704310.1016/j.lfs.2019.117043.
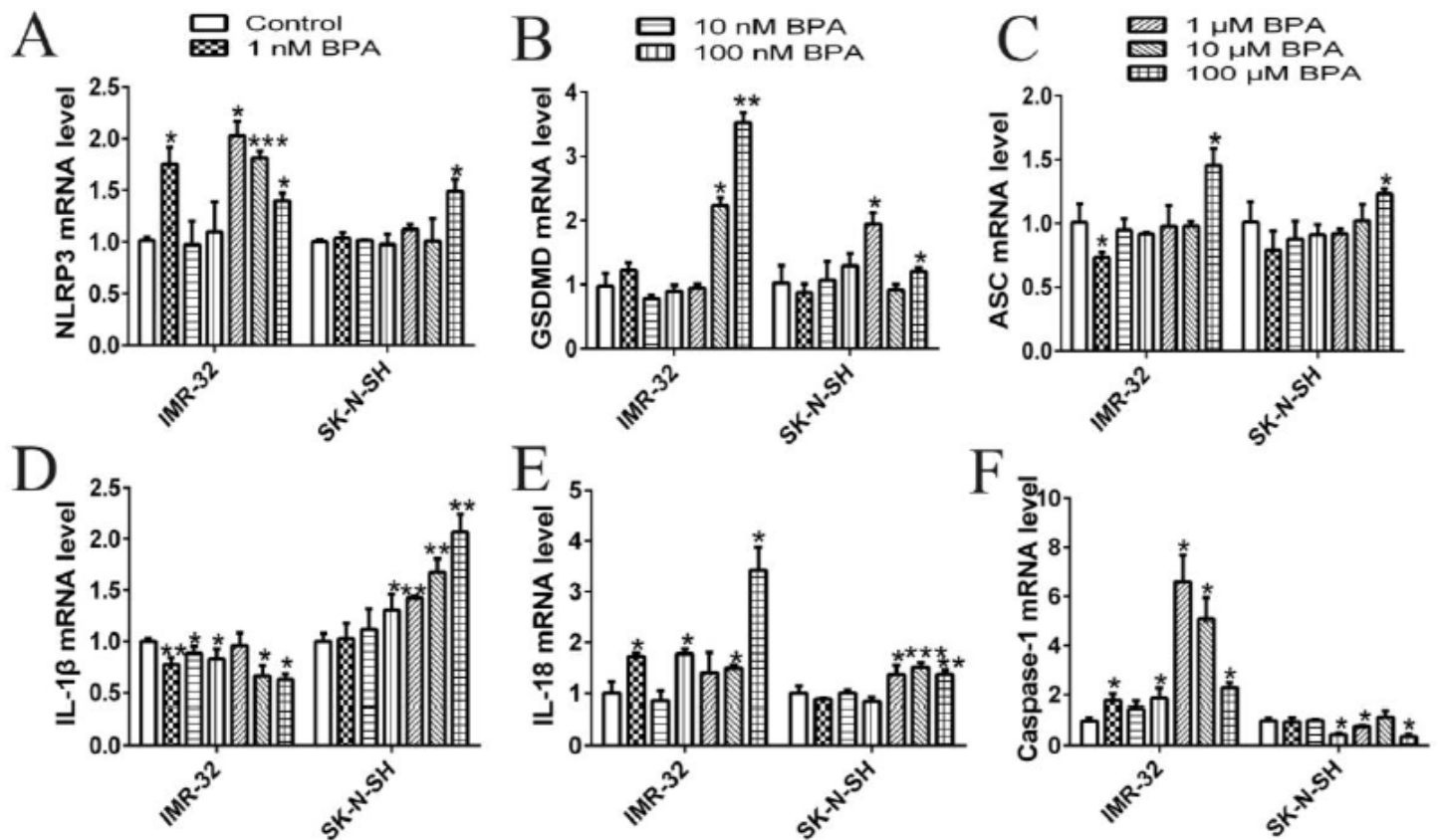
Figures

Figure 1

Effects of BPA (control, 1 nM, 10 nM, 100 nM, 1 µM, 10 µM and 100 µM) treatments for 24 h on the expressions of pyroptosis-related genes mRNA in IMR-32 and SK-N-SH cells. (A-F) Expressions of NLRP3, GSDMD, ASC, IL-1β, IL-18 and Caspase-1 mRNA compared with β-action. Data are represented as mean ± SEM (n = 3). "*" indicates significant difference compared to its corresponding control (*p < 0.05, **p < 0.01 and ***p < 0.001).
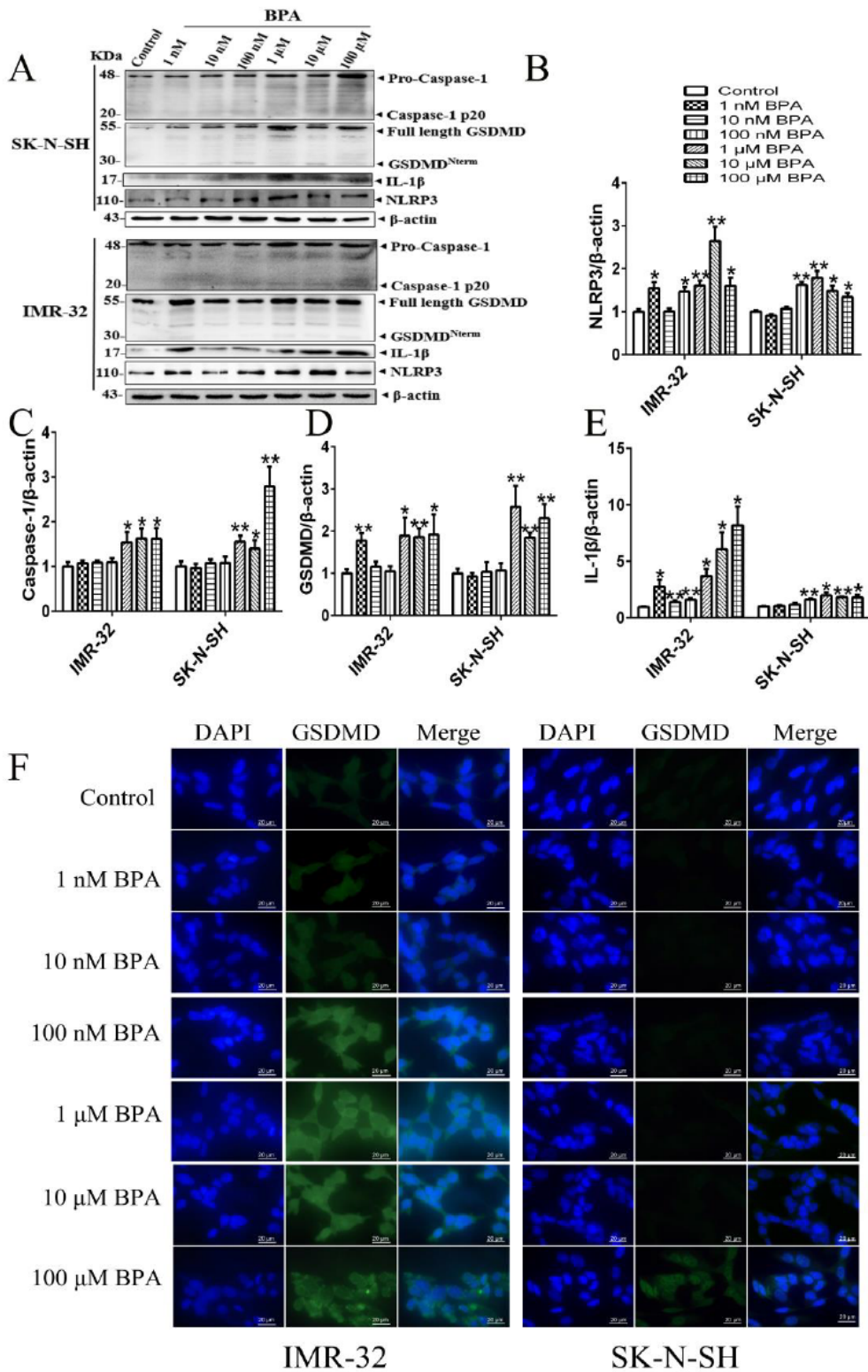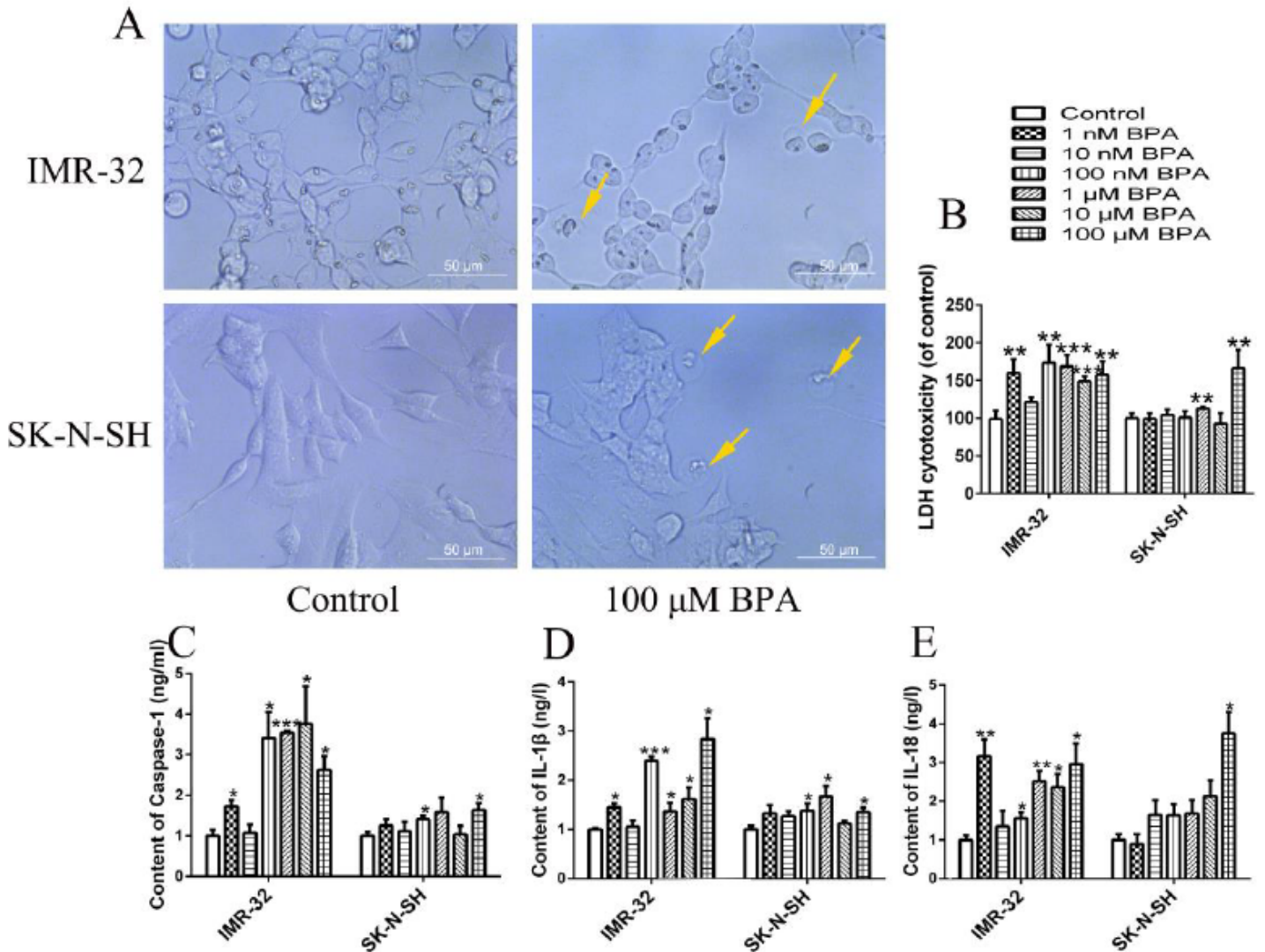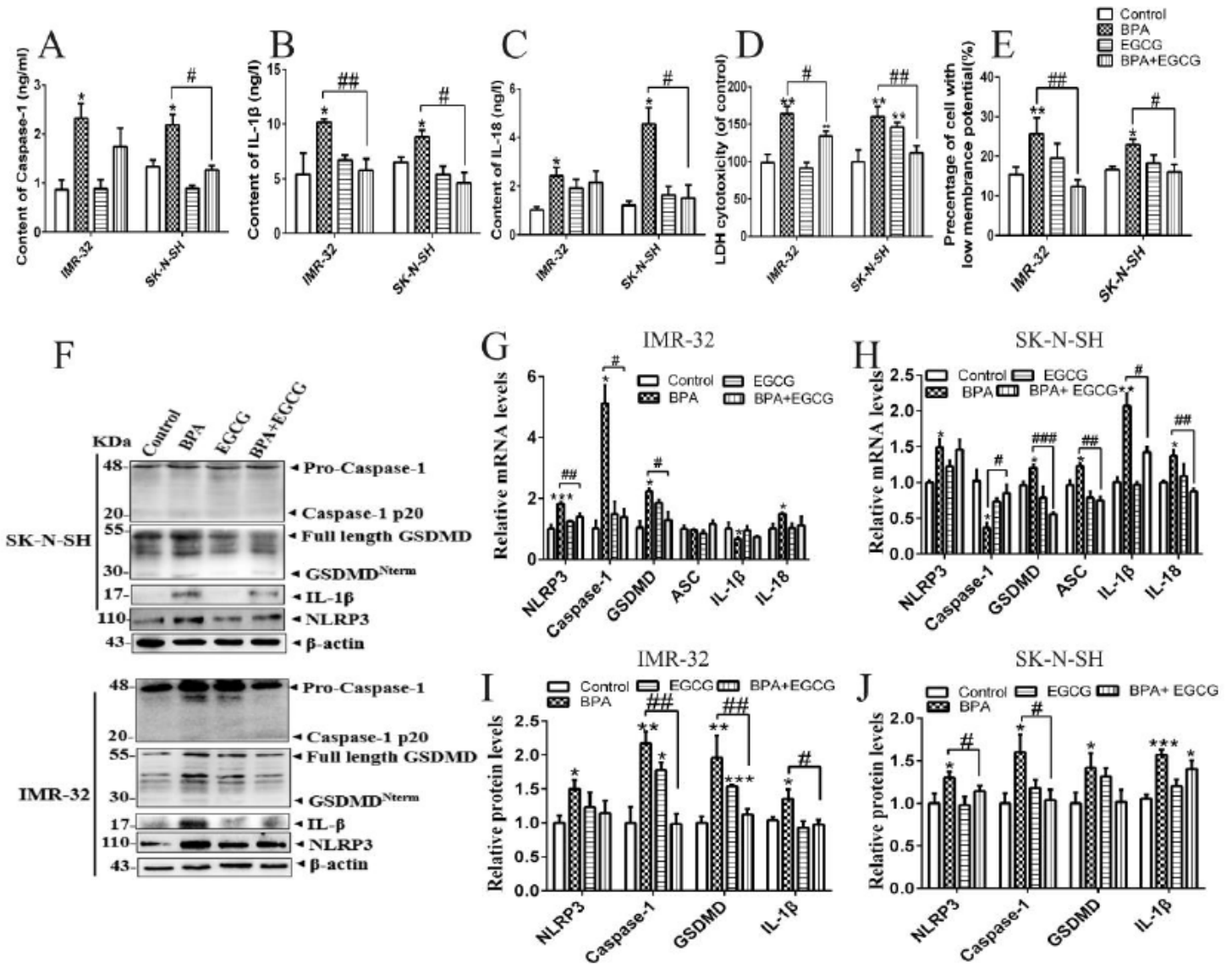

Figure 2

Effects of BPA (control, 1nM, 10 nM, 100 nM, 1 µM, 10 µM and 100 µM) treatments for 24 h on the expressions of pyroptosis-related proteins in IMR-32 and SK-N-SH cells and the cellular localization of GSDMD by immunostaining. (A) Protein band diagram. (B-E) Protein levels of NLRP3, Caspase-1, GSDMD and IL-1β compared with β-action. (F) After 24 h BPA-treatments, the distribution of GSDMD in IMR-32 and SK-N-SH cells is detected by immunofluorescent labeling of GSDMD (green) and DAPI (blue). Data are represented as mean ± SEM (n = 3). "*" indicates significant difference compared to the corresponding control (*p < 0.05, **p < 0.01 and ***p < 0.001).
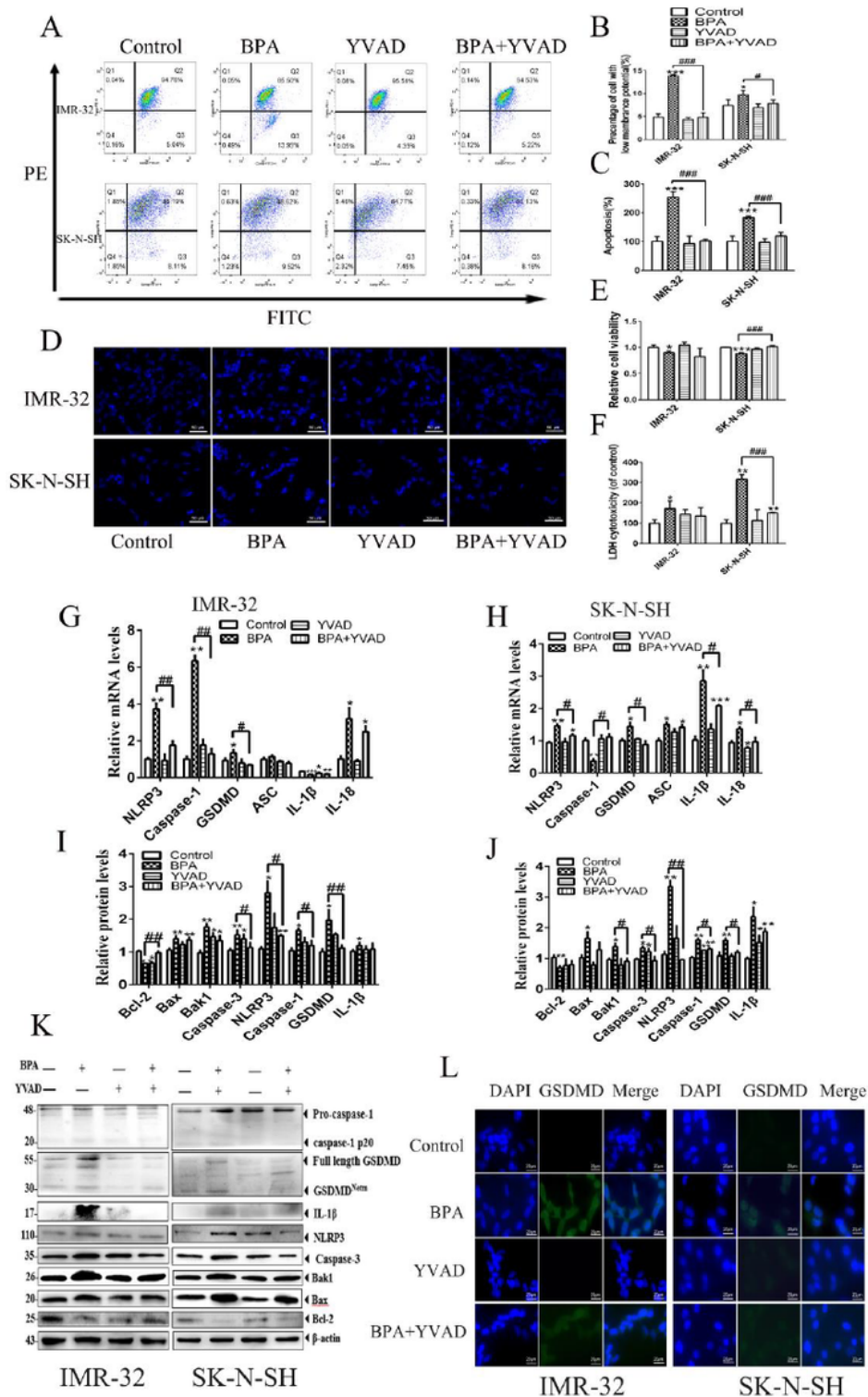

Figure 3

Morphologic alterations of IMR-32 and SK-N-SH cells and the contents of pyroptosis-related protein in supernatants. (A) Images of IMR-32 and SK-N-SH cells treated with BPA. Arrows indicate pyroptotic cells. (B) Effects of BPA (control, 1 nM, 10 nM, 100 nM, 1 µM, 10 µM and 100 µM) on the levels of LDH in supernatants. (C-E) Effects of BPA (control, 1 nM, 10 nM, 100 nM, 1 µM, 10 µM and 100 µM) on the contents of pyroptosis-related protein in supernatants for 24 h treatment. "*" indicates significant difference compared to its corresponding control (*p < 0.05, **p < 0.01 and ***p < 0.001).

Figure 4

EGCG treatments decrease the BPA-induced pyrotosis in IMR-32 and SK-N-SH cells. (A-D) Levels of Caspase-1, IL-1β, IL-18 and LDH in supernatants. (E) Cell percentages with low MMP. (F) Protein band diagram. (G-H) Effects of BPA (i.e., 10 μM and 100 μM) and EGCG (i.e., 4 μM and 8 μM) on the mRNA expressions of the pyroptosis-related genes NLRP3, Caspase-1, GSDMD, ASC, IL-1β and IL-18 in IMR-32 and SK-N-SH cells. (I-J) Protein levels of NLRP3, Caspase-1, GSDMD and IL-1β compared with β-action. The results were achieved based on at least three repeated experiments. "*" indicates the significant difference between the control and treated groups (*p < 0.05, **p < 0.01 and ***p < 0.001). "#" indicates the significant difference between two corresponding groups (#p < 0.05, ##p < 0.01 and ###p < 0.001).

Figure 5

Caspase-1 deletion attenuates the pyroptosis and mitochondrial apoptosis in IMR-32 and SK-N-SH cells. (A) Flow cytometry images of MMP. (B) Cell percentages with low MMP. (C) The apoptosis rates were significantly decreased after the inhibition of Caspase-1 receptor. (D) Hoechst staining of IMR-32 and SK-N-SH cells. (E) Cell viabilities of IMR-32 and SK-N-SH cells. (F) LDH levels in supernatants. (G) Effects of 10 μM BPA and 1 μM YVAD on the mRNA expressions of pyroptosis-related genes NLRP3, Caspase-1,

GSDMD, ASC, IL-1β and IL-18 in IMR-32 cell. (H) Effects of 100 μM BPA and 10 μM YVAD on the mRNA expressions of the pyroptosis-related genes NLRP3, Caspase-1, GSDMD, ASC, IL-1β and IL-18 in SK-N-SH cell. (I-K) Protein levels of Bcl-2, Bax, Bak1, Caspase-3, NLRP3, Caspase-1, GSDMD and IL-1β compared with β-action. (L) Immunofluorescent labeling of GSDMD (green) and DAPI (blue) demonstrates the distribution of GSDMD in IMR-32 and SK-N-SH cells. The results were achieved based on at least three repeated experiments. "*" indicates the significant difference between the control and treated groups (*p < 0.05, **p < 0.01 and ***p < 0.001). "#" indicates the significant difference between two corresponding groups (#p < 0.05, ##p < 0.01 and ###p < 0.001).
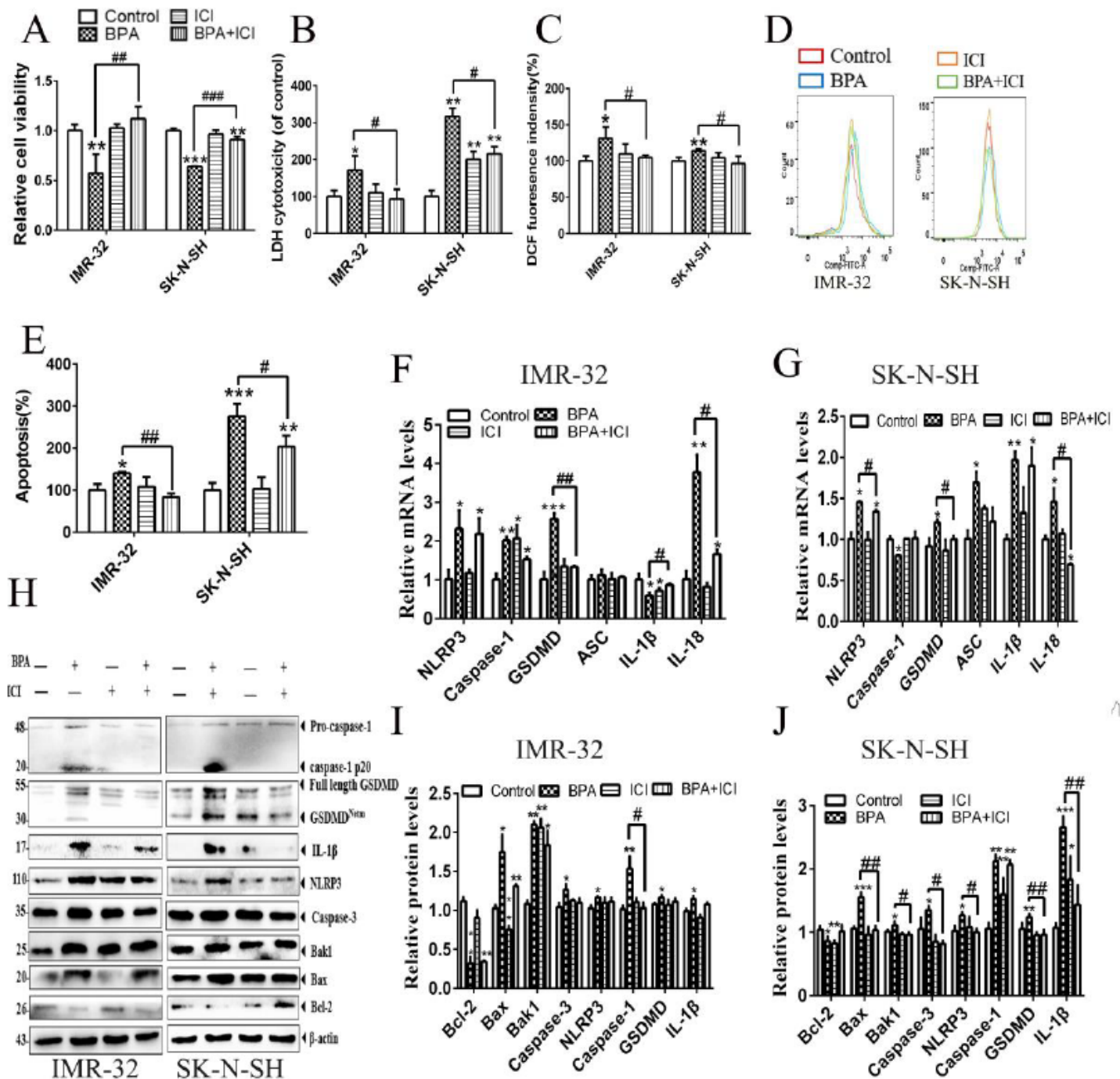

Figure 6

BPA-induced ROS production, apoptosis and pyroptosis via an estrogen-like pathway in IMR-32 and SK-N-SH cells. (A) Cell viabilities of IMR-32 and SK-N-SH cells. (B) LDH levels in supernatants. (C-D) ROS production. (E) Apoptosis rates of IMR-32 and SK-N-SH cells. (G-H) Effects of BPA (i.e., 10 μM and 100 μM) and ICI (i.e., 100 nM and 3 μM) on the mRNA expressions of the pyroptosis-related genes NLRP3, Caspase-1, GSDMD, ASC, IL-1β and IL-18 in IMR-32 and SK-N-SH cells. (F, I-J) Protein levels of Bcl-2, Bax, Bak1, Caspase-3, NLRP3, Caspase-1, GSDMD and IL-1β compared with β-action. The results were achieved based on at least three repeated experiments. "*" indicates the significant difference between the control and treated groups (*$p < 0.05$, **$p < 0.01$ and ***$p < 0.001$). "#" indicates the significant difference between two corresponding groups (#$p < 0.05$, ##$p < 0.01$ and ###$p < 0.001$).